High-Efficient Deep-Blue Light-Emitting Diodes by Using High Quality $Zn_xCd_{1-x}S/ZnS$ Core/Shell Quantum Dots

Huaibin Shen, Xianwei Bai, Aqiang Wang, Hongzhe Wang, Lei Qian, Yixing Yang, Alexandre Titov, Jake Hyvonen, Ying Zheng, and Lin Song Li**

High-quality violet-blue emitting $Zn_xCd_{1-x}S/ZnS$ core/shell quantum dots (QDs) are synthesized by a new method, called "nucleation at low temperature/shell growth at high temperature". The resulting nearly monodisperse $Zn_xCd_{1-x}S/ZnS$ core/shell QDs have high PL quantum yield (near to 100%), high color purity (FWHM) <25 nm), good color tunability in the violet-blue optical window from 400 to 470 nm, and good chemical/photochemical stability. More importantly, the new well-established protocols are easy to apply to large-scale synthesis; around 37 g $Zn_xCd_{1-x}S/ZnS$ core/shell QDs can be easily synthesized in one batch reaction. Highly efficient deep-blue quantum dot-based light-emitting diodes (QD-LEDs) are demonstrated by employing the $Zn_xCd_{1-x}S/ZnS$ core/shell QDs as emitters. The bright and efficient QD-LEDs show a maximum luminance up to 4100 cd m^{-2}, and peak external quantum efficiency (EQE) of 3.8%, corresponding to 1.13 cd A^{-1} in luminous efficiency. Such high value of the peak EQE can be comparable with OLED technology. These results signify a remarkable progress, not only in the synthesis of high-quality QDs but also in QD-LEDs that offer a practicle platform for the realization of QD-based violet-blue display and lighting.

1. Introduction

The unique photoluminescence (PL) and electroluminescence (EL) properties of inorganic semiconductive quantum dots (QDs) make them important for both fundamental research and industrial applications, such as light-emitting diodes (LEDs), lasers, biomedical labeling, and so forth.[1–7] Especially because of their high quantum efficiency, highly saturated color, and simple color tunability in the solid state compared to those of conjugated molecules (polymers) or inorganic phosphors, QDs are considered one of the most promising emitters for next-generation displays and solid-state lighting.[5–19] However, the fabrication of highly efficient quantum dot-based light-emitting devices (QD-LEDs) has a demand on high quality QDs.[19,20] With the renovating of synthetic methods, QDs with high quantum yields (QYs) have been continuously developed, and their corresponding performances of QD-LEDs have been improved rapidly. Such as, the highest luminance of red emitted QD-LEDs can reach up to 50 000 cd m^{-2}, and the external quantum efficiency (EQE) can reach above 18%.[20] The green QD-LEDs also show a brightness over 200 000 cd m^{-2} with EQE of 5.8%.[16] All of those values are comparable with state-of-the-art organic light-emitting diodes (OLED) technology which indicates that the QD-LEDs have more potential for applications towards display and solid-state lighting.[16,20] The results of red and green QD-LEDs all give attentions to brightness and efficiency, but for the blue and deep-blue QD-LEDs, the highest EQE just reached 1.7% with the luminance of 2250 cd m^{-2}.[16] Most recently, we have reported blue QD-LEDs with the highest luminance values (4700 cd m^{-2}) by using $Zn_{1-x}Cd_xS_{1-y}Se_y/ZnS$ core/shell QDs as emitters, but the EQE is only 0.8% which is much lower than OLED. For $Zn_{1-x}Cd_xS_{1-y}Se_y/ZnS$ core/shell QDs, although the QY can reach up to 75% in blue-green area, it is difficult to get high QY (>70%) in deep-blue area.[17] The reasons for low efficiency of blue and deep-blue QD-LEDs due to larger potential energy barrier at the interface of blue QDs and hole transport layer, and the lower QY of blue QDs is a relative critical factor.

In the past, most of the synthesis of QDs with violet-blue emission is mainly focused on CdS based core/shell QDs and their QYs were lower than 65%.[21,22] Even though, there are a few studies based on CdSe or ZnCdSe core/shell QDs,[23,24] and the QYs of these reports were still less than 75%. The researches on CdSe related QDs with violet-blue emission is yet not optimistic. With maximized small size effect, the extremely small CdSe QDs capped with protective ZnS shell only showed the highest QY of 50%.[23] Compared to the previously reported red and green QDs that showed QYs up to 90%,[25–27] there is still more room to improve the QYs of violet-blue QDs. So it is really attractive to find a way to synthesize QDs with violet-blue

Dr. H. Shen, X. Bai, A. Wang, H. Wang, L. Qian, Prof. L. S. Li
Key Laboratory for Special Functional Materials of Ministry of Education
Henan University
Kaifeng, 475004, P. R. China
E-mail: lsli@henu.edu.cn
Dr. Y. Yang, A. Titov, J. Hyvonen, Y. Zheng
NanoPhotonica, Inc. 747 SW 2nd Ave.
Gainesville, FL, 32601, USA
E-mail: ying.zheng@nanophotonica.com

DOI: 10.1002/adfm.201302964

emission, high stability, and high QYs (>90%). It not only has vital significance for the synthesis but also for improving the performance of violet-blue QD-LEDs.

So far, for the synthesis of core/shell QDs, the most common way is higher temperature nucleation and lower temperature shell growth.[28–32] Herein, we present a new method which utilizes high temperature injection for the synthesis of QD cores and an even higher temperature for shell growth to obtain new violet-blue emission core/shell QDs that show high QYs near to 100% as well as high photostability. Three points of this work should be emphatically emphasized: 1) Pre-screening of QDs cores for the synthesis of core/shell QDs. To get high-quality $Zn_xCd_{1-x}S$/ZnS core/shell QDs with different PL positions, we choose the corresponding highest quality (i.e., the highest QYs) $Zn_xCd_{1-x}S$ as core; 2) Near unity high QYs with highly saturated color purity and wide tunable emission in whole blue range. The resulting nearly monodisperse $Zn_xCd_{1-x}S$/ZnS core/shell QDs yielded from our approach show the best PL QY near to 100%, high color purity (with full width at half-maximum (FWHM) <25 nm), good color tunability in the violet-blue optical window from 400 to 470 nm, and good chemical/photochemical stability; and 3) Validated high performance in lighting-emitting devices. Violet-blue LEDs based on $Zn_xCd_{1-x}S$/ZnS core/shell QDs have been successfully demonstrated by using our optimized structure for QD-LEDs. Highly bright violet-blue QD-LEDs showing a maximum luminance up to 4100 cd m^{-2}, and peak EQE of 3.8%, corresponding to 1.13 cd A^{-1} in luminous efficiency, which can be comparable with state-of-the-art OLED technology, this results give attentions to both brightness and efficiency. These results signify a remarkable progress not only in the synthesis of high-quality blue colloidal QDs but also in QD-LEDs which offer a practicable platform for the realization of QD-based full-color display and lighting.

2. Results and Discussion

2.1. Synthesis of $Zn_xCd_{1-x}S$/ZnS Core/Shell QDs

Generally, high quality core QDs are needed for the synthesis of high quality core/shell QDs due to the QYs and monodispersity of core/shell QDs depend on the core quality in a sense.[29] Therefore, a pre-selection of high quality $Zn_xCd_{1-x}S$ QDs with the highest QY as cores to make core/shell QDs is a "must-have" process. To obtain different range of blue emissions, $Zn_xCd_{1-x}S$ alloy QDs can be continuously tuned by changing the reaction time and the ratio of Zn to Cd. From the PL spectra of $Zn_xCd_{1-x}S$ core QDs with different x value (**Figure 1**), it is clearly demonstrated that the PL emissions are tunable between 400 nm and 475 nm and narrow FWHMs between 18–25 nm were obtained. An obviously red shift of PL was observed during the growth of $Zn_xCd_{1-x}S$ QDs. During the whole reaction process, the PL QYs is varied from 19 to 30%. The highest QYs related to different Zn and Cd ratio may appears at different reaction time which are shown as blue curves in Figure 1.

During the growth process of shell materials, the PL emissions were drastically enhanced. The PL QY of core-shell QDs was measured near to 100%, which is the highest solution based value among those of blue emitting QDs reported so far. The synthetic strategy of $Zn_xCd_{1-x}S$/ZnS core/shell QDs is shown in **Scheme 1**. **Figure 2**a shows the absorption and PL spectra of $Zn_xCd_{1-x}S$/ZnS (x = 0.25) core/shell QDs taken at different reaction time. PL spectra shift to longer wavelengths compared to that of the original cores in the first 15 min of the reaction (from 445 to 449 nm). Such red shift has also been observed in several other multishell QDs and indicates the extension of wave function into the shell region, which increases the effective size of the core and reduces the quantum confinement effect by the semiconductor wave function.[24,29] It also reveals

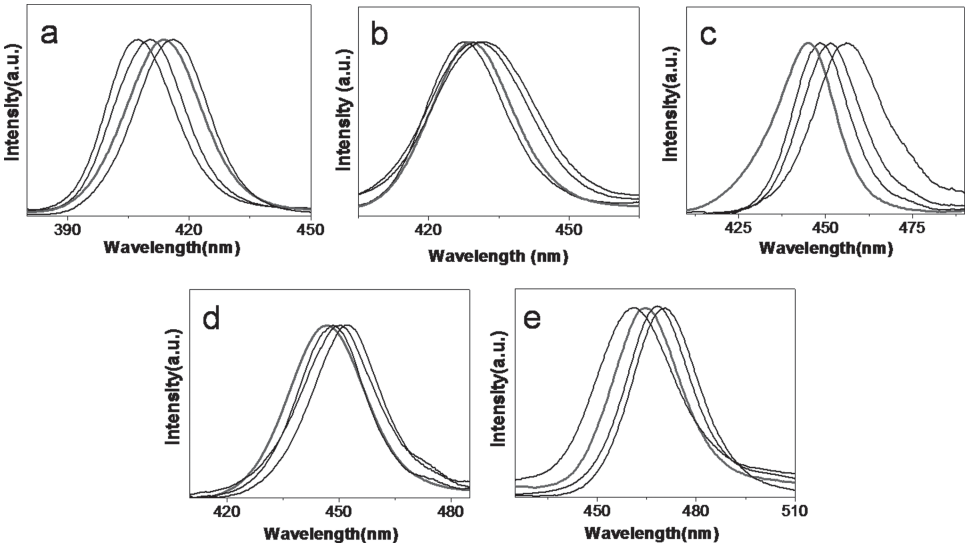

Figure 1. Photoluminescence spectra of $Zn_xCd_{1-x}S$ core QDs with different molar ratios of Zn and Cd. a) $x = 0.66$; b) $x = 0.5$; c) $x = 0.25$; d) $x = 0.2$; e) $x = 0.1$. From the left to the right of the reaction time is: 5 min; 15 min; 30 min; and 1 h. Blue curves represent the highest QYs for every fixed Zn and Cd ratios.

that the absorption and PL spectra show slight blue shift from 15 min to the end of the reaction (from 449 to 441 nm). Similar phenomenon was observed before when CdSe QDs were covered with a composite $CdS/Cd_{0.5}Zn_{0.5}S/ZnS$-shell, and this spectral shift was attributed to partial formation of alloy shells.[29] At the same time, the FWHM of PL decreased greatly from 23.6 nm (at 15 min of the reaction) to 19.7 nm (at the end of the reaction), as shown in Figure 2a. This result is consistent with the decrease of size distribution of the QDs. The narrow PL FWHM may be due to the slow shell precursor infusion and the low reactivity of the octanethiol, which may provide a constant and sufficient monomer production rate and is consistent with recent research.[27,33] A series of $Zn_xCd_{1-x}S/ZnS$ QDs dispersed in hexanes with tunable PL emission in the range of 400–470 nm is shown in Figure 2b. This covers most part of the violet-blue window which is very important for the applications of deep-blue LEDs. More importantly, the PL QY of the core/shell QDs can reach near to 100%.

There are four proposed reasons for the obtaining of core/shell QDs with such high QYs: 1) Core selection process for the synthesis of core/shell QDs. To get high-quality of $Zn_xCd_{1-x}S/ZnS$ core/shell QDs with different PL emissions, high quality $Zn_xCd_{1-x}S$ QDs were sifted out for cores. 2) The more matching lattice constants of $Zn_xCd_{1-x}S$ with ZnS shell material than CdS. Because of highly matched lattice constants between $Zn_xCd_{1-x}S$ core and ZnS shell, the structure of $Zn_xCd_{1-x}S/ZnS$ core/shell can largely reduce the surface tension and thus minimize the formation of interface defects.[30] 3) The successful surface passivation of the cores with more wider band gap materials. When the wide band gap ZnS shells are grown onto relative narrower band gap $Zn_xCd_{1-x}S$ core QDs, both the electrons and the holes are mostly confined to the core region, which provides a great improvement for the PL QYs.[24] 4) The growth of shell materials with high temperatures. Different from traditional nucleation at high temperature/shell growth at low temperature method,[28–32] our preparation approach adopted shell growth at a high temperature level. The high growth temperature promoted the quick growth of shells, and more, the S and Zn atoms might diffuse into the $Zn_xCd_{1-x}S$ core regions, so the surface of $Zn_xCd_{1-x}S$ cores could also be restored and a consecutive change of lattice parameters could be formed with $Zn_xCd_{1-x}S$ buffer layers, and the stress defects were avoided.[27] It also revealed the reason for a little PL blue-shift when more outer layers of ZnS were coated onto $Zn_xCd_{1-x}S$ QDs.

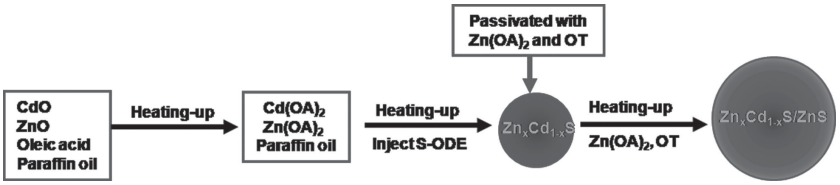

Scheme 1. The synthetic procedure of $Zn_xCd_{1-x}S/ZnS$ core/shell QDs.

For the synthesis of core/shell QDs, not only PL QYs should be considered but also stability.[30] It is well known that the optical properties of QDs are extremely sensitive to their surface chemistry and chemical environment. The coordinating organic ligands used to passivate the QDs' surface during growth are one of the strong contributors to its optical properties, especially the emission efficiency.[24] Although there was a high QY when thin shells were overcoated, but the stability was still low.[30] To improve the PL stability, a thick shell is needed indeed. But after growing of thicker shells, the QY declined gradually due to the accumulation of structural defects. Based on the previous study of the effect of shell thickness on the optical stability properties, we designed QDs with the shell-thickness of ≈9.5 monolayers to ensure the core/shell QDs with high QYs and high stability.[30] The $Zn_xCd_{1-x}S/ZnS$ core/shell QDs were insensitive to the ligand loss (Figure S1, Supporting Information) and showed a very high photochemical stability (Figure S1 inset). More importantly, the new well-established protocols are easy to do large-scale synthesis and 37 g of high quality alloyed $Zn_xCd_{1-x}S/ZnS$ core/shell QDs can be easily synthesized in one batch reaction (Figure S2, Supporting Information).

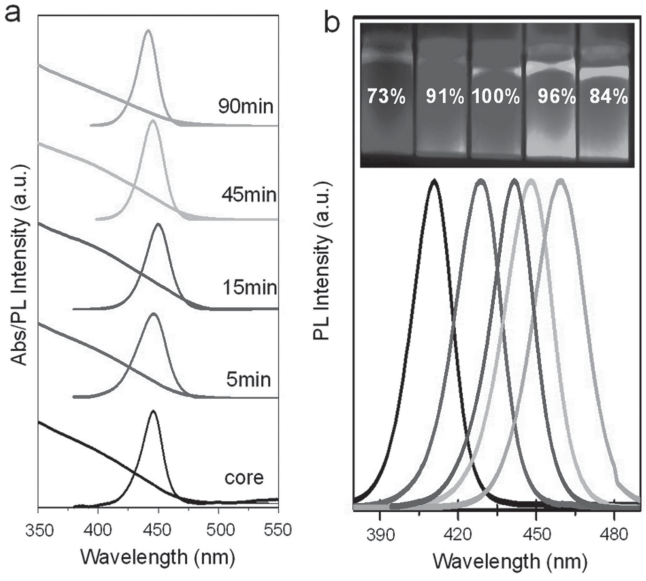

Figure 2. a) Evolution of the absorption and PL spectra upon consecutive growth of $Zn_xCd_{1-x}S/ZnS$ (x = 0.25) core/shell QDs. b) Normalized PL spectra (λ_{ex} = 360 nm) of $Zn_xCd_{1-x}S/ZnS$ core/shell QDs starting from $Zn_xCd_{1-x}S$ core with different x and representative UV-illuminated photos of $Zn_xCd_{1-x}S/ZnS$ core/shell QDs dispersion in hexanes.

2.2. Morphology and Structure of $Zn_xCd_{1-x}S/ZnS$ Core/Shell QDs

TEM and HRTEM images of $Zn_xCd_{1-x}S$ (x = 0.25) cores and $Zn_xCd_{1-x}S/ZnS$ (x = 0.25) core/shell QDs are shown in **Figure 3**. The TEM images show reasonable size distributions with average diameters of b) 5.7 nm, c) 6.5 nm, d) 8.4 nm, and e) 10.8 nm, respectively. These values are all based on the original core QDs with a mean diameter of 4.8 nm (a). The corresponding HRTEM images of $Zn_xCd_{1-x}S$ cores and core/shell

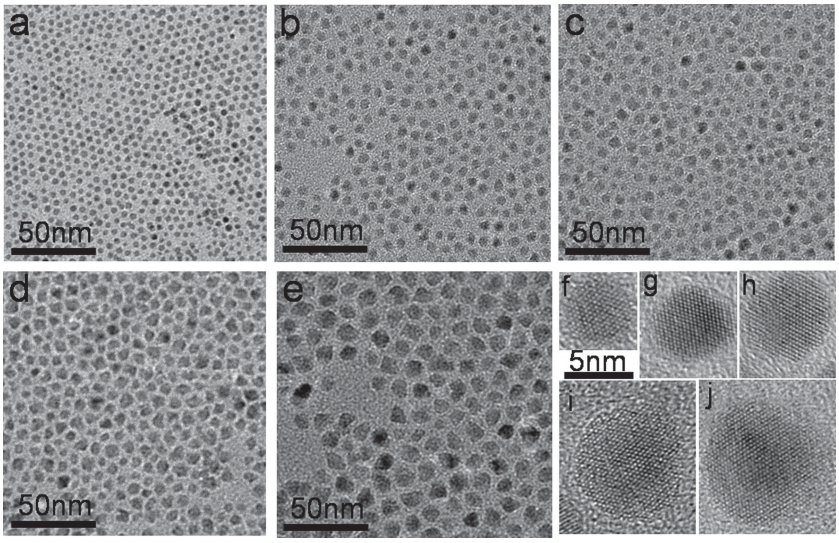

Figure 3. TEM and HRTEM (inset) images of the $Zn_xCd_{1-x}S$ (x = 0.25) cores and $Zn_xCd_{1-x}S$/ZnS (x = 0.25) core/shell QDs obtained under typical reaction conditions. a) TEM images of $Zn_xCd_{1-x}S$ cores; b) growth shell for 5 min; c) growth shell for 15 min; d) growth shell for 45 min; e) growth shell for 90 min. f–j) the corresponding HRTEM of (a–e).

QDs are shown in Figure 3f–j. There is no evidence for the presence of interface between the core and shell and all the HRTEM images show high crystallinity with continuous lattice fringes throughout the whole QDs which implies that the growth of shells occurs in the regime of coherent epitaxy.[28] As shown in the HRTEM image of $Zn_xCd_{1-x}S$/ZnS QD (Figure 3j), the distance between two adjacent planes is 0.31 nm, which corresponds to the (002) plane of the hexagonal phase ZnS. To further characterize the evolution of structures of $Zn_xCd_{1-x}S$/ZnS core/shell QDs, XRD patterns were used to determine the crystallographic properties (**Figure 4**). According to the XRD patterns, the peak positions of $Zn_xCd_{1-x}S$ (x = 0.25) QDs lie between the bulk wurtzite CdS (JCPDS: 80–0006) and wurtzite ZnS (JCPDS: 80–0007). This indicates that the XRD peaks of these samples are not derived from a mixture of CdS and ZnS which suggests the compositional homogeneity of $Zn_xCd_{1-x}S$ QDs. It is also clearly shown that XRD peaks get narrower along with the increase of shell thickness, which indicates the increase of the QDs' sizes. An obvious peak shift to standard wurtzite phase ZnS position has been observed when ZnS shells were grown on the wurtzite phase $Zn_xCd_{1-x}S$ cores and all samples still kept hexagonal structures.

2.3. Fabrication of Blue Emitting LEDs using $Zn_xCd_{1-x}S$/ZnS Core/Shell QDs as Emitters

Based on this efficient synthesis method and resultant high quality blue QDs phosphor, we further explored the potential application of $Zn_{1-x}Cd_xS$/ZnS (x = 0.25) core/shell QDs as emitters in deep-blue QD-LEDs. Based on our recently published results,[15] multiple monolayers of QDs are needed for efficient recombination of electrons and holes directly in the QD emissive layer. Here, we adopted a similar device structure with multiple QD layers as emissive layers to study the performance of those core/shell QDs with blue PL emissions. The structure of the QD-LEDs is schematically shown in **Figure 5**a. The QD-LEDs were fabricated with layers of indium tin oxide (ITO)/poly (ethylenedioxythiophene):polystyrene sulphonate (PEDOT:PSS) (40 nm)/poly[9,9-dioctylfluorene-co-N-[4-(3-methylpropyl)]-diphenylamine] (TFB) (30 nm)/$Zn_{1-x}Cd_xS$/ZnS core/shell QDs (20 nm)/ZnO NPs (25 nm)/Al to confine exciton formation within the QD layer. Such device structure and parameters for every layer are adopted from our previous report with a little modification of using TFB to replace Poly-TPD.[15] Since TFB possesses an even lower HOMO level than Poly-TPD, the insertion of TFB layer will doubtless reduce the barrier for the hole injection from polymers into QDs. All layers are spin-coated onto the pattered ITO substrate except for the Al cathode, which is deposited through vacuum thermal evaporation. It has been reported that the use of orthogonal solvents for adjacent layers can successfully avoid physical damage of films caused by sequential casting processes in such multilayer structures.[15]

The schematic energy level diagram of the QD-LEDs is shown in Figure 5b. The ZnO nanoparticle (NP) layer provides

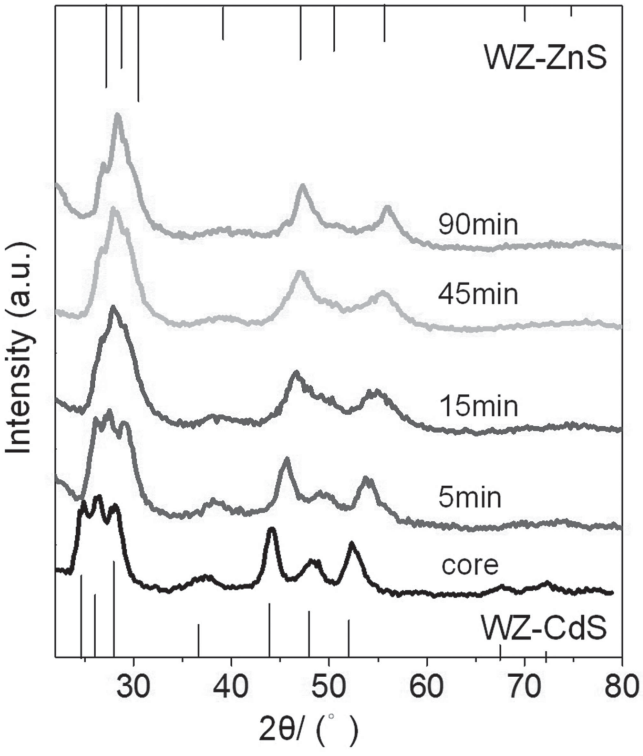

Figure 4. Powder XRD patterns of $Zn_xCd_{1-x}S$ (core), and $Zn_xCd_{1-x}S$/ZnS core/shell QDs with different growth time. For comparison, the standard powder diffraction patterns of wurtzite -CdS (JCPDS, 80–0006), and wurtzite -ZnS (JCPDS, 80–0007) are provided.

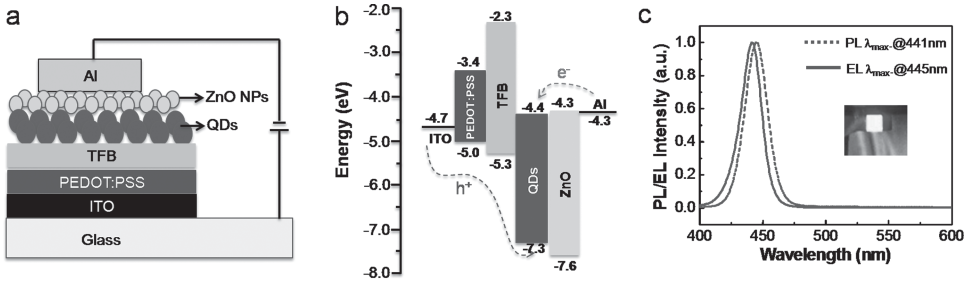

Figure 5. a) Schematic of layers in the device structure. b) Energy level diagram for the various layers. c) Normalized photoluminescence spectra (solid lines) and EL (dashed lines) spectra of blue-green QD-LEDs. The energy levels for materials are cited from the literature.[13,15,34–36]

efficient electron injection channel as well as a hole blocking layer due to the valence band offset at the QD/ZnO nanoparticle interface, leading to improved charge recombination efficiency.[15] PL spectra of $Zn_{1-x}Cd_xS/ZnS$ core/shell QDs and the electroluminescence (EL) spectra of the corresponding QD-LEDs are shown in Figure 5c. The EL peak of the blue QD-LEDs was at wavelength of 445 nm with a narrow EL FWHM (<30 nm) at a slightly red-shifted wavelength relative to their corresponding PL measured in the chloroform solution.[37]

The current density–luminance–voltage (*J*–*L*–*V*) characteristics, current efficiency and external quantum efficiency curves for the deep-blue QD-LEDs were shown in **Figure 6**a–c. The deep-blue QD-LED (EL peak = 445 nm) based on our $Zn_xCd_{1-x}S/ZnS$ (x = 0.25) core/shell QDs shows an high brightness over 4100 cd m^{-2} (Figure 6a), which is comparable with the highest value ever reported for QD-based light-emitting diodes,[26] but show an unprecedentedly EQE which reaches up to 3.8% which give attentions to both brightness and efficiency (Figure 6b), and this results is close to the state-of-the-art OLED (4–6%) technology.[38] The significant improvement compared to previous reports due to the high QYs of the $Zn_{1-x}Cd_xS/ZnS$ core/shell QDs and the excellent structure of QD-LEDs. The main factors that affect the external quantum efficiencies of QD-LEDs can be concluded as the carrier transport/injection and recombination efficiencies.[7,14,15,19] In the case of effects of charge transport/injection rates on QD-LEDs, the appropriate choices of TFB and ZnO assisted the matching of hole/electron injection through the optimized device structure and energy band alignment. For the blue QD of $Zn_xCd_{1-x}S$, high QY means high recombination efficiencies.

In addition, as talked to the external quantum efficiencies, it has been observed that a relatively thin shell of up to 7 monolayers (2.4 nm) can significantly suppress single-QDs blinking and contribute to high photoluminescence QYs.[27] We believe that a shell thickness of 3 nm for QDs adopted here can dramatically minimize the emission intermittency and thus alleviate QD charging related blinking under electrical bias. ZnO NP layer not only provides efficient electron injection from the Al cathode into $Zn_{1-x}Cd_xS/ZnS$ QDs, but also helps to confine holes within the QD layer due to the valence band offset at the QD/ZnO NP interface, leading to an improved charge recombination efficiency.[15] So in this structure the injection of electrons and holes into $Zn_{1-x}Cd_xS_{1-y}S/ZnS$ core/shell QDs enables the balanced exciton formation and efficient exciton recombination within QD active layers and leads to high efficiency and brightness. The turn-on voltages and peak luminous efficiency are 2.3 V and 1.13 cd A^{-1}, respectively, for our blue QD-LEDs (Figure 6b). All these results indicate that the $Zn_{1-x}Cd_xS/ZnS$ core/shell QDs are suitable for making blue QD-LEDs just as CdSe/CdS and CdSe/ZnS QDs are more suitable for the production of red and green QD-LED.[16,20]

3. Conclusions

We have synthesized high-quality violet-blue emitting $Zn_xCd_{1-x}S/ZnS$ core/shell QDs by high temperature shell growth method. The resulting nearly monodisperse $Zn_xCd_{1-x}S/ZnS$ core/shell QDs yielded from our approach with high PL quantum yield (near to 100%), high color purity (FWHM < 25 nm), good color tunability in the violet-blue optical window from 400 to 470 nm.

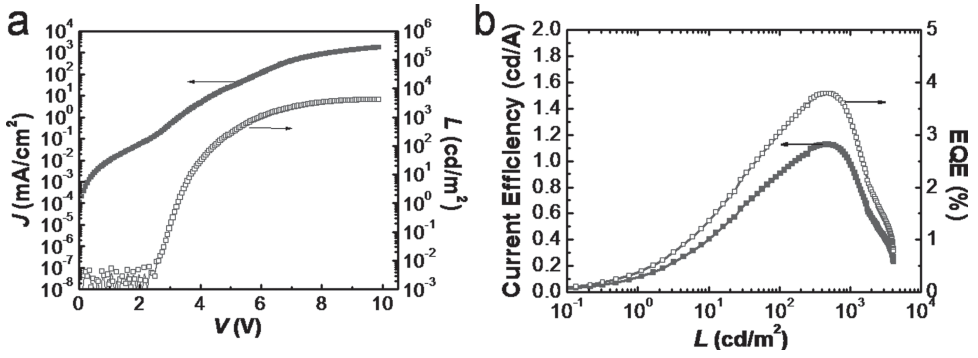

Figure 6. Electroluminescence performance of QD-LEDs with blue emission. a) Current–density (*J*) and luminance (*L*) versus driving voltage (*V*). b) Current efficiency and EQE versus luminance.

Up to 37 g of high quality alloyed $Zn_xCd_{1-x}S/ZnS$ core/shell QDs can be easily synthesized in one batch reaction. Highly efficient blue light-emitting diodes (LEDs) have also been demonstrated by employing the $Zn_xCd_{1-x}S/ZnS$ core/shell QDs as emitters. Highly bright and efficient blue QD-LEDs showing maximum luminance up to 4100 cd m^{-2} and peak EQE of 3.8% are demonstrated. These results signify a remarkable progress not only in the large-scale synthesis of high-quality colloidal QDs but also in QD-LEDs that offer a practicable platform for the realization of QD-based violet-blue display.

4. Experimental Section

Chemicals: All reagents were used as received without further experimental purification. Cadmium oxide (CdO, 99.99%), zinc oxide (ZnO, 99.9%, powder), sulfur (S, 99.998%, powder), 1-octadecene (ODE, 90%), 1-octanethiol (OT, 98%), and oleic acid (OA, 90%) were purchased from Aldrich. Paraffin (analytical grade), acetone (analytical grade), hexanes (analytical grade), and methanol (analytical grade) were obtained from Beijing Chemical Reagent Co., Ltd, China.

Typical Synthesis of $Zn_xCd_{1-x}S/ZnS$: As a typical synthetic procedure, 0.4 mmol of CdO, 0.1 mmol of ZnO, 15 mL of paraffin oil and 1 mL of OA were placed in a 100 mL round flask. The mixture was heated to 150 °C, degassed under 0.1 Torr pressure for 20 min, filled with N_2gas, and further heated to 300 °C to form a clear mixture solution of $Cd(OA)_2$ and $Zn(OA)_2$. At this temperature, 0.5 mmol of S powder dissolved in 2 mL of ODE was quickly injected into the reaction flask. Samples were extracted to monitor their PL spectra. The growth of shell started when the QY of core reached the highest value. For the shell growth reaction, the reaction solution was heated to 310 °C under nitrogen flow and magnetic stirring, and a desired amount of $Zn(OA)_2$ (10 mmol of ZnO mixed with 15 mL of oleic acid and 5 mL of paraffin was heated to 300 °C to form a clear mixture solution under N_2 flow.) and octanethiol (1.2 equivalent amounts refer to $Zn(OA)_2$, diluted in 5 mL ODE) began to be injected dropwise into the reaction solution at a rate of 6 mL h^{-1} using a syringe pump. After finishing precursor infusion, the solution was further annealed at 310 °C for 30 min. After the reaction was completed, the temperature was cooled down to room temperature and the QDs were purified using acetone or methanol.

Fabrication of QD-LEDs: QD-LEDs were fabricated on patterned ITO coated glass substrates and the processes are similar to that reported in our previously published reports.[15,17] In short, the cleaned ITO glass substrates were spin-coated with PEDOT:PSS (AI 4083) and baked at 150 °C for 15 min in air and were then transferred to a N_2-filled glove box for spin-coating of the TFB, QDs, and ZnO NP layers. ZnO NP were obtained from NanoPhotonica, Inc. and used after filtered with 0.45 um PVDF filter. The TFB solution (1.5 wt% in chlorobenzene) and spin-coating process of 2000 rpm for 30 s followed by baking at 110 °C for 30 min were used for the hole-transport TFB layer. QDs (≈10 mg mL^{-1}, toluene) and ZnO NPs (30 mg mL^{-1}, ethanol) were spin-coated with spin speed of 1000 rpm and 4000 rpm to achieve layer thickness of ≈20 nm and ≈25 nm, respectively. The top Al cathode (100 nm thick) was then deposited to form an active device area of 4 mm^2.

Characterization: Room temperature UV-vis absorption and PL spectra were measured with an Ocean Optics spectrophotometer (mode PC2000-ISA). PL quantum yields (QYs) were determined by comparison of the integrated fluorescence intensity of the QD samples in solution with that of standard of known QYs (LD 423, QY = 68% in ethanol). Transmission electron microscopy (TEM) studies were performed using a JEOL JEM-2010 electron microscope operating at 200 kV. Phase determination of the products was carried out on an X-ray diffractometer (Philips X' Pert Pro) using Cu-Ka radiation (wavelength = 1.54 Å). Current–luminance–voltage characteristics were measured using an Agilent 4155C semiconductor parameter analyser with a calibrated Newport silicon diode. The luminance was calibrated using a Minolta luminance meter (LS-100). The electroluminescence spectra were obtained with an Ocean Optics high-resolution spectrometer (HR4000) and a Keithley 2400 power source.

Supporting Information

Supporting Information is available from the Wiley Online Library or from the author.

Acknowledgements

This work was financially supported by the research project of the National Natural Science Foundation of China (21071041 and 21201055), Program for Changjiang Scholars and Innovative Research Team in University (No. PCS IRT1126), and the Scientific Research Foundation of Henan University (2012ZRZD08). Supporting Information is available online from Wiley InterScience or from the author.

Received: August 24, 2013
Revised: November 1, 2013
Published online: December 16, 2013

[1] V. I. Klimov, A. A. Mikhailovsky, S. Xu, A. Malko, J. A. Hollingsworth, C. A. Leatherdale, H. J. Eisler, M. G. Bawendi, *Science* **2000**, *290*, 314.
[2] G. D. Scholes, *Adv. Funct. Mater.* **2008**, *18*, 1157.
[3] W. C. W. Chan, S. M. Ni, *Science* **1998**, *281*, 2016.
[4] J. Tang, E. H. Sargent, *Adv. Mater.* **2011**, *23*, 12.
[5] V. L. Colvin, M. C. Schlamp, A. P. Alivisatos, *Nature* **1994**, *370*, 354.
[6] S. Coe, W.-K. Woo, M. G. Bawendi, V. Bulović, *Nature* **2002**, *420*, 800.
[7] Q. Sun, Y. A. Wang, L. S. Li, D. Wang, T. Zhu, J. Xu, C. Yang, Y. Li, *Nat. Photonics* **2007**, *1*, 717.
[8] J. M. Caruge, J. E. Halpert, V. Wood, V. Bulović, M. G. Bawendi, *Nat. Photonics* **2008**, *2*, 247.
[9] J. S. Steckel, P. Snee, S. Coe, J. P. Zimmer, J. E. Halp ert, P. Anikeeva, L. Kim, V. Bulović, M. G. Bawendi, *Angew. C hem. Int. Ed.* **2006**, *45*, 796.
[10] J. Zhao, J. A. Bardecker, A. M. Munro, M. S. Liu, Y. Niu, I. Ding, J. Luo, B. Chen, A. K. Y. Jen, D. S. Ginger, *Nano Lett.* **2006**, *6*, 463.
[11] B. Chen, H. Zhong, W. Zhang, Z. Tan, Y. Li, C. Yu, T. Zhai, Y. Bando, S. Yang, B. Zou, *Adv. Funct. Mater.* **2012**, *22*, 2081.
[12] K.-S. Cho, E. K. Lee, W.-J. Joo, E. Jang, T.-H. Kim, S. J. Lee, S.-J. Kwon, J. Y. Han, B.-K. Kim, B. L. Choi, J. M. Kim, *Nat. Photon.* **2009**, *3*, 341.
[13] W. K. Bae, J. Kwak, J. W. Park, K. Char, C. Lee, S. Lee, *Adv. Mater.* **2009**, *21*, 1690.
[14] a) V. Wood, V. Bulović, *Nano Rev.* **2010**, *1*, 1; b) S. Coe-Sullivan, J. S. Steckel, W. K. Woo, M. G. Bawendi, V. Bulović, *Adv. Funct. Mater.* **2005**, *15*, 1117.
[15] L. Qian, Y. Zheng, J. Xue, P. H. Holloway, *Nat. Photonics* **2011**, *5*, 543.
[16] J. Kwak, W. K. Bae, D. Lee, I. Park, J. Lim, M. Park, H. Cho, H. Woo, D. Y. Yoon, K. Char, S. Lee, C. Lee, *Nano Lett.* **2012**, *12*, 2362.
[17] H. Shen, S. Wang, H. Wang, J. Niu, L. Qian, Y. Yang, A. Titov, J. Hyvonen, Y. Zheng, L. S. Li, *ACS Appl. Mater. Interfaces* **2013**, *5*, 4260.
[18] B. N. Pal, Y. Ghosh, S. Brovelli, R. Laocharoensuk, V. I. Klimov, J. A. Hollingsworth, H. Htoon, *Nano Lett.* **2012**, *12*, 331.
[19] Y. Shirasaki, G. J. Supran, M. G. Bawendi, V. Bulović, *Nat. Photonics* **2013**, *7*, 13.
[20] B. S. Mashford, M. Stevenson, Z. Popovic, C. Hamilton, Z. Zhou, C. Breen, J. Steckel, V. Bulović, M. G. Bawendi, S. Coe-Sullivan, P. T. Kazlas, *Nat. Photonics* **2013**, *7*, 407.

[21] D. Chen, F. Zhao, H. Qi, M. Rutherford, X. Peng, *Chem. Mater.* **2010**, *22*, 1437.
[22] W. Zhang, H. Zhang, Y. Feng, X. Zhong, *ACS Nano* **2010**, *6*, 11066.
[23] R. Capek, K. Lambert, D. Dorfs, P. F. Smet, D. Poelman, A. Eychmuller, Z. Hens, *Chem. Mater.* **2009**, *21*, 1743.
[24] H. Shen, C. Zhou, S. Xu, C. Yu, H. Wang, X. Chen, L. S. Li, *J. Mater. Chem.* **2011**, *21*, 6046.
[25] H. S. Jang, H. Yang, S. W. Kim, J. Y. Han, S. G. Lee, D. Y. Jeon, *Adv. Mater.* **2008**, *20*, 2696.
[26] S. Jun, E. Jang, *Angew. Chem. Int. Ed.* **2013**, *52*, 679.
[27] O. Chen, J. Zhao, V. P. Chauhan, J. Cui, C. Wong, D. K. Harris, H. Wei, H.-S. Han, D. Fukumura, R. K. Jain, M. G. Bawendi, *Nat. Mater.* **2013**, *12*, 445.
[28] B. O. Dabbousi, J. Rodriguez-Viejo, F. V. Mikulec, J. R. Heine, H. Mattoussi, R. Ober, K. F. Jensen, M. G. Bawendi, *J. Phys. Chem. B* **1997**, *101*, 9463.
[29] R. Xie, U. Kolb, J. Li, T. Basché, A. Mews, *J. Am. Chem. Soc.* **2005**, *127*, 7480.
[30] S. Xu, H. Shen, C. Zhou, H. Yuan, C. Liu, H. Wang, L. Ma, L. S. Li, *J. Phys. Chem. C.* **2011**, *115*, 20876.
[31] J. I. Kim, J.-K. Lee, *Adv. Funct. Mater.* **2006**, *16*, 2077.
[32] Y. Chen, J. Vela, H. Htoon, J. L. Casson, D. J. Werder, D. A. Bussian, V. I. Klimov, J. A. Hollingsworth, *J. Am. Chem. Soc.* **2008**, *130*, 5026.
[33] M. D. Clark, S. K. Kumar, J. S. Owen, E. M. Chan, *Nano Lett.* **2011**, *11*, 1976.
[34] W. K. Bae, J. Kwak, J. Lim, D. Lee, M. K. Nam, K. Char, C. Lee, S. Lee, *Nanotechnology* **2009**, *20*, 075202.
[35] W. J. E. Beek, M. M. Wienk, R. A. J. Janssen, *Adv. Mater.* **2004**, *16*, 1009.
[36] H. H. Fong, J. Lee, Y. Lim, A. A. Zakhidov, W. W. H. Wong, A. B. Holmes, C. K. Ober, G. G. Malliaras, *Adv. Mater.* **2011**, *23*, 735.
[37] C. R. Kagan, C. B. Murray, M. G. Bawendi, *Phys. Rev. B* **1996**, *54*, 8633.
[38] A. Mikami, Y. Nishita, Y. Iida, *SID Symp. Dig. Tech. Papers* **2006**, *37*, 1376.